Med Ultrason 2023, Vol. 25, no. 1, 111-121

Echocardiography in the detection of lead-related infective endocarditis

Tina Bečić, Vedran Carević, Ružica Perković-Avelini, Damir Fabijanić

Department of Cardiology, University Hospital of Split, Split, Croatia

To the Editor,

A 70-year-old man with a permanent pacemaker (PM) implanted 10 years ago was admitted because of a febrile state. During the 7 months period before admission, he was febrile four times up to 39°C, lasting several days with general weakness, pain in the back and legs, and accelerated erythrocyte sedimentation rate and elevated C-reactive protein recorded, while blood and urine cultures were sterile. Each time he was treated empirically with antibiotics with short-term improvement.

Two-dimensional transthoracic echocardiography (2DTTE) indicated a possible mass in the right atrium (fig 1a). Two and three-dimensional transoesophageal echocardiography (2DTEE and 3DTEE) revealed mass on the atrial segment of ventricular lead (fig 1b,c); the segment of the lead which passes through the tricuspid valve and surrounding cardiac structures were free of the infection (fig 1d). *Staphylococcus aureus* was isolated from the blood culture. After 4 weeks of antibiotic treatment, the patient underwent a successful extraction of the PM system.

Lead-related infective endocarditis (LRIE) is a serious infectious disease developing in patients with cardiac implantable electronic devices (CIED) [1]. Its specific sign is vegetation, a mobile oscillating mass attached to the CIED lead, which in combination with positive blood cultures meet a major Duke criterion [1].

2DTTE is the primary imaging technique in the case of suspected lead vegetation(s), but with poor sensitivity and specificity for their diagnosis and evaluation of the spread of infection to surrounding cardiac structures [2]. Therefore, 2DTEE is indicated in all patients with suspicion of LRIE [1]. A 2DTEE probe which directs the ultrasound plane through a 180-degree arc effectively provides a panoramic image of 360-degree heart structures. However, a detailed 2DTEE inspection is hampered by reverberations and artifacts generated by the electrodes which make identification of vegetation(s) near these structures difficult [2]. 3DTEE provides a clear, fast and detailed anatomical image in real time providing additional information about the appearance of the electrode and its passage through the tricuspid orifice. Compared to 2DTEE, 3DTEE enables a better visualization of the lead(s) and surrounding cardiac structures and the detec-

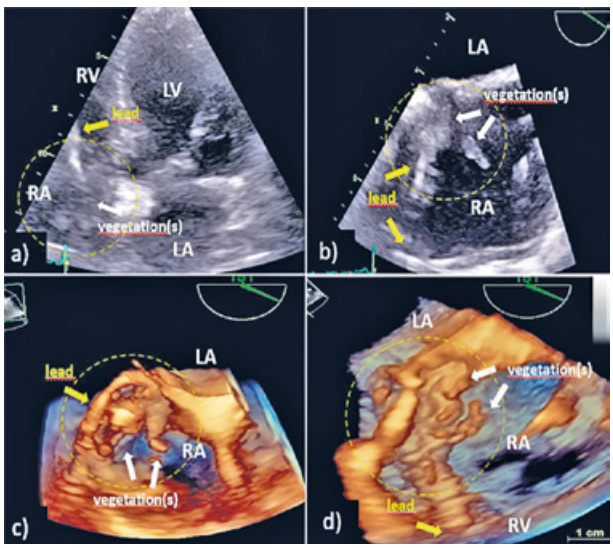

Fig 1. 2DTTE indicates a possible mass in the right atrium (a); 2DTEE reveals a hypoechoic mobile mass on the atrial segment of the ventricular lead (b); 3DTEE confirmed large vegetations on the atrial segment of the ventricular lead (c); the lead segment passing through the tricuspid valve and the surrounding cardiac structures were free of infection (d).

Received 11.12.2022 Accepted 15.01.2023
Med Ultrason
2023, Vol. 25, No 1, 111-112, DOI: 10.11152/mu-4002,
Corresponding author: Damir Fabijanic
Department of Cardiology,
University Hospital of Split,
21000 Split, Croatia
E-mail: damirfabijanic62@gmail.com

tion of additional vegetations that are often overlooked using 2DTEE [2]. Most importantly, 3DTEE allows a detailed anatomical description of the location, size, shape, and consistency of the vegetation, necessary to evaluate the possibility and the best time for lead extraction, as a mandatory therapeutic intervention in patients with LRIE [1].

References

1. Polewczyk A, Jachec W, Tomaszewski A, et al. Lead-related infective endocarditis: factors influencing the formation of large vegetations. Europace 2017;19:1022-1030.
2. Almomani A, Siddiqui K, Ahmad M. Echocardiography in patients with complications related to pacemakers and cardiac defibrillators. Echocardiography 2014;31:388-399.

EUS-guided drainage for pancreatic duct stone combined with main pancreatic duct stenosis after pancreaticoduodenectomy: a case report

Hongfei He, Tingting Yu, Yaoting Li, Senlin Hou, Lichao Zhang

Biliopancreatic Endoscopic Surgery Department, The Second Hospital of Hebei Medical University, Shijiazhuang, China

To the Editor,

The incidence of pancreaticojejunostomy anastomotic stricture has been reported in about 5% after pancreaticoduodenectomy [1], but the main pancreatic duct stenosis is extremely rare in such cases.

An 81-year-old woman was admitted with epigastric pain for two weeks, and the patient had undergone pancreaticoduodenectomy for ampullary cancer 8 years ago. MRCP showed abnormal small nodules in the pancreatic duct and peripancreatic inflammatory exudation. We prepared ERCP using balloon-assisted enteroscopy but pancreaticojejunostomy anastomotic could not be found. So, we chose endoscopic ultrasound and the scan showed that the pancreatic duct in the body of the pancreas was dilated and with strong echoes in the interior. A puncture needle was inserted into the dilated pancreatic duct and fluoroscopy was performed showing the stone and the narrow pancreatic duct at the site of the stone incarceration, which made the antegrade intervention for the stone become complex. We placed a fully covered metal stent to connect the pancreatic duct and the intestinal lumen for drainage and expand the narrow pancreatic duct, a double pigtail plastic stent being placed in the fistula. The patient was discharged after the abdominal pain disappeared. The patient was hospitalized again 4 months later. We used duodenoscopy to find the double pigtail plastic stent, and the guidewire was inserted into the pancreatic duct through the fistula. Fluoroscopy showed that the narrow pancreatic duct had been dilated. After the stents were removed with forceps, the antegrade intervention for the stone was successfully performed through the fistula with a balloon (fig 1).

Faced with patients of pancreaticojejunostomy anastomotic stricture, the rendezvous technique or ERCP using balloon-assisted enteroscopy is preferred, but the absolute requirement for both techniques is that endoscopy can always advance to the anastomosis site [2]. For this case, unobstructed drainage of the pancreatic duct was the most important. The elastic tension of the fully covered metal stent could expand the stenosis and provide operation space for the antegrade intervention.

References

1. Fujigaki S, Shiomi H, Atalla H, et al. EUS-guided drainage for a non-dilated pancreatic duct using a re-puncture technique in a patient with stricture-related pancreatitis (with video). J Hepatobiliary Pancreat Sci 2021;28:e54-e55.

Received 21.11.2022 Accepted 15.01.2023
Med Ultrason
2023, Vol. 25, No 1, 112-113, DOI: 10.11152/mu-3960,
Corresponding author: Lichao Zhang
Biliopancreatic Endoscopic Surgery Department, The Second Hospital of Hebei Medical University, CN050000, Shijiazhuang, Hebei province, China
E-mail: zhang.lichao@163.com

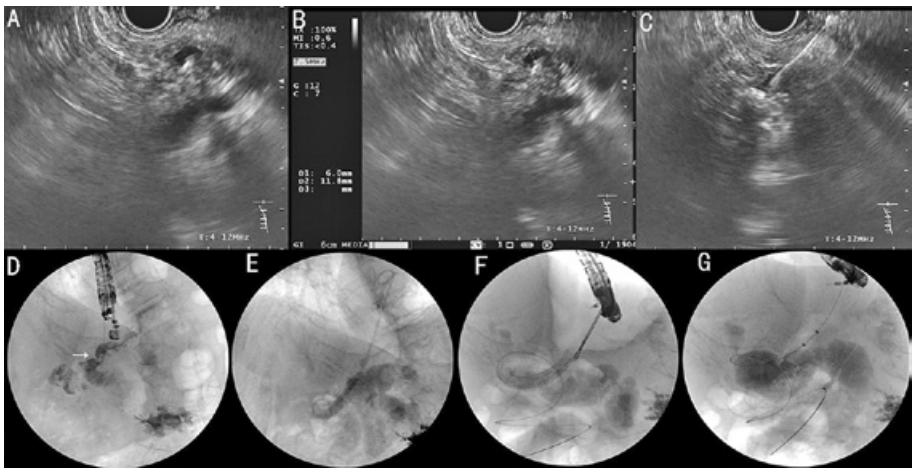

Fig 1. A. Endoscopic ultrasound showed the pancreatic duct stone in the body of the pancreas; B. Measurement of pancreatic duct diameter and puncture distance under endoscopic ultrasound; C. The puncture needle was inserted into the dilated pancreatic duct; D. Fluoroscopy showed the stone and the narrow pancreatic duct at the site of the stone incarceration; E. A fully covered metal stent and a double pigtail plastic stent was placed; F. Removing the stents with forceps; G. The antegrade intervention for the stone was successfully performed through the fistula with a balloon.

2. Katanuma A, Hayashi T, Kin T, et al. Interventional endoscopic ultrasonography in patients with surgically altered anatomy: Techniques and literature review. Dig Endosc 2020;32:263-274.

Right atrial thrombosis and lymphoblastic leukemia

Fenglin Jiang[1], Caijun Han[2]

[1]Department of Medical Ultrasound, [2]Department of Clinical Laboratory, Yanbian University Hospital, Yanji, Jilin, China

To the Editor,

A 44-year-old man was diagnosed with acute Ph^+ B-lymphocyte leukemia for 3 years. Two years ago, he received umbilical cord blood stem cell transplantation and CD19/CD22 bi-target CAR-T therapy. He was treated with oral dasatinib since then. This time, the patient came

Received 22.12.2022 Accepted 06.02.2023
Med Ultrason
2023, Vol. 25, No 1, 113-114, DOI: 10.11152/mu-4017,
Corresponding author: Fenglin Jiang
Department of Medical Ultrasound,
Yanbian University Hospital,
#1327 Juzi St.
Yanji 133000, China
Phone: +86-433-2660056
E-mail: jiangfenglin@sina.com

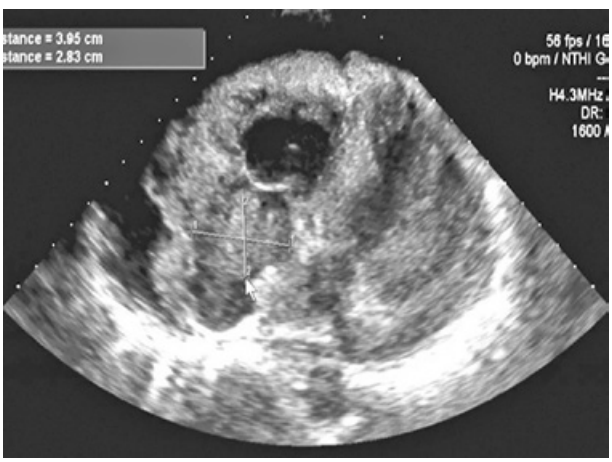

Fig 1. Echocardiography, four-chamber section showed a 39.5x28.3 mm hypoechoic mass in the right atrium,and a large amount of pericardial effusion.

to the hospital with chest tightness, with white blood cell count of 12.53x10^9/L and neutrophil count of 8.91x10^9/L. Neutrophils 71.10%, lymphocytes 17.5%, monocytes 11.30%, hemoglobin 106 g/L, platelets 237x10^9/L. Echocardiography showed a large amount of pericardial effusion. A 39.5x28.3mm weak echo light mass was seen in the right atrium, and thrombus was considered (fig 1).

The main research fields of OncoCardiology include common risk factors and interventions of cardiovascular diseases and tumors, cardiovascular complications caused by anti-tumor treatment, cardiac tumors and tumors combined with cardiovascular diseases. Cardiovascular disease and tumors have become the two diseases with the highest incidence rate. Hematologic diseases occur in a series of diseases around hemorrhage and thrombosis. The common symptoms of leukemia are fever, infection and hemorrhage.

Right atrial thrombosis is a rare, but potentially serious complication of acute lymphoblastic leukemia treatment. In the Jarvis et al study, 11 (2.7%, 95%CI 1.4-4.9) of 406 patients had asymptomatic right atrial thrombosis, ranging from 10 to 25 mm at detection [1]. Bonanni et al believed that the right atrial mass in patients with T-cell chronic lymphoblastic leukemia was an abnormal mechanism of thrombosis [2].

Reference

1. Jarvis KB, Andersson NG, Giertz M, et al. Asymptomatic Right Atrial Thrombosis After Acute Lymphoblastic Leukemia Treatment. J Pediatr Hematol Oncol 2021;43:e564-e566.
2. Bonanni L, Adami F, Angelini A, et al. Images in cardiovascular medicine. Right atrial mass in a patient with T-cell chronic lymphocytic leukemia: an unusual mechanism of thrombus formation. Circulation 2007;116:e569-e572.

Evaluation and subsequent treatment for superficial peroneal entrapment and hypertrophic scar using high-resolution ultrasound

Chia-Yu Kuo[1], Kuo-Chang Wei[1,2]

[1]Department of Physical Medicine and Rehabilitation, Cathay General Hospital, [2]Department of Physical Medicine and Rehabilitation, National Taiwan University Hospital, Taipei, Taiwan

To the Editor,

A 31-year-old healthy female presented with a left ankle hypertrophic scar and paresthesia after exposure to a traffic accident. In addition, the patient also experienced paresthesia at the left anterolateral ankle, innervated by the superficial peroneal nerve (SPN).

High-resolution ultrasonography (HRUS) was performed to investigate the integrity of SPN and possible SPN entrapment neuropathy. A linear transducer was firstly placed 5 cm proximal to the lateral malleolus to localize the SPN at the horizontal plane between the peroneus brevis and extensor digitorum longus (EDL) (fig 1a). The transducer was subsequently moved caudally, and a gradual approximation of the SPN and scar tissue was noted. The scar tissue was a hypoechoic ovoid mass located superficially to the crural fascia. Eventually, the SPN was compressed underneath the scar tissue (fig 1b). US-guided hydrodissection and nerve block were performed on the SPN at the site where the SPN was about to go beneath the scar (fig 1c). After waiting for 5 min to allow the local anesthetic to work, echo-guided steroid injection with 10 mg of triamcinolone was performed at the longitudinal plane of the scar (fig 1d).

This report showed the value of HRUS in the diagnosis of peripheral nerve pathologies. Although electrodiagnostic studies may provide important physiological

Received 11.12.2022 Accepted 15.01.2023
Med Ultrason
2023, Vol. 25, No 1, 114-115, DOI: 10.11152/mu-3997,
Corresponding author: Kuo-Chang Wei, MD
Department of Physical Medicine and Rehabilitation, Cathay General Hospital
280, Renai Rd., Da-an Dist.,
Taipei City 106, Taiwan (R.O.C.)
E-mail: gordon80446@gmail.com
Phone: 886-972278198

information, they are painful and incapable of providing structural information. HRUS on the other hand provides additional morphological information on the injured nerve [1]. In this case, the hypertrophic scar made the recording of the sensory nerve action potential of the SPN inaccurate. Therefore, we used HRUS to perform nerve tracking for the SPN to check the integrity of the nerve and possible entrapment site.

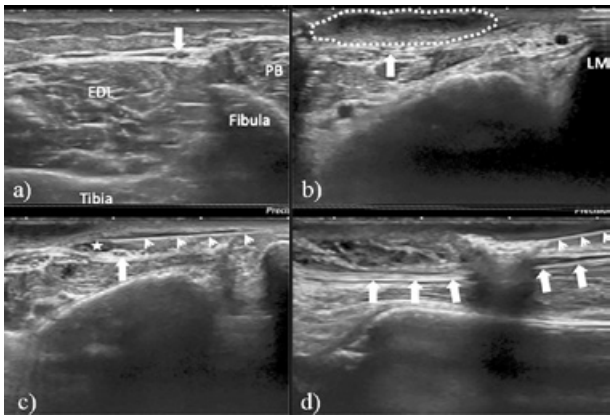

Fig 1. Ultrasound nerve tracking of the left superficial peroneal nerve (SPN) (a, b). Note the left SPN was compressed by the scar (b). After nerve tracking was performed, US-guided hydrodissection and nerve block was performed to the left SPN near the compression site (c). Subsequent ultrasound-guided intralesional steroid injection to the hypertrophic scar was performed at the longitudinal plane of the scar (d). Again, note that the SPN run right underneath the hypertrophic scar. Arrow, SPN; arrowhead, needle; asterisk, anechoic dextrose solution; circled area, hypertrophic scar; LM, lateral malleolus.

Currently, intralesional steroid injection is commonly used as first-line therapy for hypertrophic scars. Because significant procedural pain is often reported, and repeated injections are often required; methods to reduce pain are important [2]. In this case, HRUS-guided nerve block prior to intralesional steroid injection completely relieved the pain of steroid injections. In addition, unwanted neurovascular injuries during steroid injection were avoided under ultrasonography guidance.

References

1. Hsueh HW, Wei KC, Fan SP, Wu CH. Ultrasound imaging and treatment in a rare case with bilateral supinator syndrome. Med Ultrason 2022;24):250-251.
2. Morelli Coppola M, Salzillo R, Segreto F, Persichetti P. Triamcinolone acetonide intralesional injection for the treatment of keloid scars: patient selection and perspectives. Clin Cosmet Investig Dermatol 2018;11:387-396.

EUS-guided fine needle biopsy for hepatocarcinoma of the right liver lobe as a rescue diagnostic technique after a negative percutaneous-guided liver biopsy

Alina Ioana Tantau[1], Teodor Zaharie[2]

[1]4th Medical Clinic, Gastroenterology Department, [2]3rd Medical Clinic, Histopathology Department, "Iuliu Haţieganu" University of Medicine and Pharmacy, Cluj-Napoca, Romania

To the Editor,

Transjugular and percutaneous approaches are the most common techniques for liver biopsy [1]. In the last decade, endoscopic ultrasound (EUS)-tissue acquisition using fine needle aspiration (FNA) or fine needle biopsy (FNB) from left and, more recently, right lobe of the liver has been developed [2-4]. EUS-liver biopsies were compared with other techniques such as computed tomography or ultrasound (US) in terms of diagnostic accuracy of hepatic tumors [5]. The majority of the studies found similar results between those techniques with a high diagnostic accuracy varying between 90-100% [5]. Recent studies reported the utility of EUS-FNA or FNB on right liver masses [2-3]. Adequate specimen is significantly

Received 06.12.2022 Accepted 15.01.2023
Med Ultrason
2023, Vol. 25, No 1, 115-116, DOI: 10.11152/mu-3993,
Corresponding author: Alina Ioana Tantau
CF Hospital, 18, Republicii street,
400015, Cluj-Napoca
E-mail: alitantau@gmail.com

higher in the left lobe versus right lobe but technical success and diagnostic accuracy for liver masses were similar in both lobes [2-4].

We present the case of a man of 77 years old, complaining of nausea and weight loss. Physical examination revealed a large painless liver. Abdominal US examination detected a large right liver mass, more probably a hepatocarcinoma (HCC). A US-guided liver biopsy was performed with inconclusive histological examination. Therefore, we decided to perform liver biopsy guided by EUS. We used 22 gauge FNB needle (22-G Franseen-tip needle, Acquire, Boston Scientific Incorporated, Boston, Massachusetts, United States). Two passes of FNB with at least ten "back and forward" procedures per pass was performed. There were 2 tissue fragments per pass (fig 1a). Size of fragments ranged from 30-100 mm in length.

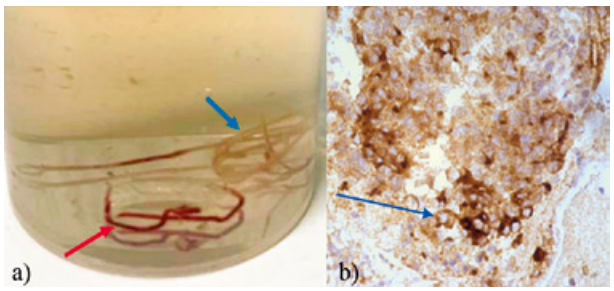

Fig 1. a) EUS-FNB liver. Macroscopic on-site evaluation. Visible core optain after EUS-FNB. The bleu arrow indicates a ten-pink core, the red arrow indicates a hemorrhagic core; b) Immunohistochemistry. Diffusely positive glypican 3 (GLY-3) staining (blue arrow), multiple 40x

The width of tissue fragments measured 0.5-0.8 mm. The positivity of MCK (citokeratin, multi), GLY (glypican-3) (fig 1b), HAS (hepatocyte specific antigen) markers and the lack of mCEA (monoclonal carcinoembryonic antigen), CD34, CD56 markers brought us to the final diagnosis of fibrolamellarhepatocarcinoma associated with virus B infection.

The EUS-guided tissue acquisition can be a suitable technique in either cirrhotic or non-cirrhotic patients with suspected HCC in order to provide an accurate histopathological diagnosis [1].

References

1. European Association for the Study of the Liver. EASL Clinical Practice Guidelines: Management of Hepatocellular carcinoma. J Hepatol 2018;69:182-236.
2. Oh D, Seo DW, Hong SM, et al. Endoscopic ultrasound-guided fine-needle aspiration can target right liver mass. Endosc Ultrasound 2017;6:109–115.
3. Zhang L, Cai Z, Rodriguez J, Zhang S, Thomas J, Zhu H. Fine needle biopsy of malignant tumors of the liver: a retrospective study of 624 cases from a single institution experience. Diag Pathol 2020;15:43 .
4. Chen F, Bao H, Deng Z, Zhao Q, Tian G, Jiang TA. Endoscopic ultrasound-guided sampling using core biopsy needle for diagnosis of left-lobe hepatocellular carcinoma in patients with underlying cirrhosis. J Cancer Res Therap 2020;16:1100-1105.
5. Pineda JJ, Diehl DL, Miao CL, et al. EUS-guided liver biopsy provides diagnostic samples comparable with those via the percutaneous or transjugular route. Gastrointest Endosc 2016;83:360–365.

Flexor hallucis brevis' trigger point and dry needling treatment: a myofascial pain syndrome perspective on big toe pain

Mustafa Hüseyin Temel[1], Elif Özyiğit[2]

[1]Physical Medicine and Rehabilitation Clinic, Üsküdar State Hospital, [2]Physical Medicine and Rehabilitation Clinic, Kanuni Sultan Süleyman Training and Research Hospital, İstanbul, Turkey

Received 14.12.2022 Accepted 15.01.2023
Med Ultrason
2023, Vol. 25, No 1, 116-117, DOI: 10.11152/mu-3987,
Corresponding author: Mustafa Hüseyin Temel
Clinic of Physical Medicine and Rehabilitation, Üsküdar State Hospital, İstanbul, Turkey
Phone: +90 216 474 79 00
E-mail: mhuseyintemel@gmail.com

To the Editor,

One of the most common areas of the foot to experience pain is the big toe joint, also known as the first metatarsophalangeal joint. Pain frequently manifests gradually over a period of years, but it can also strike suddenly as a result of an injury [1]. The pain in the big toe negatively

Fig 1. Positioning of the ultrasound probe and ultrasound-guided needling of the flexor hallucis brevis muscle: a) positioning of the utrasound probe; b) ultrasound-guided needling of the flexor hallucis brevis muscle (FHB: Flexor Hallucis Brevis, MTH: Metatarsal Head, ADHO: Adductor Obliquus Hallucis)

affects quality of life, regardless of the underlying pathology [2]. Myofascial pain syndrome (MPS) is one of the most frequent and overlooked causes of musculoskeletal pain, which is a result of the myofascial trigger points (MTrPs) that are located in muscle tissue [3]. The flexor hallucis brevis is an essential muscle that may have MTrP when examining patients with big toe pain [4,5]. It is difficult to diagnose when the MTrP of this muscle, which should be considered in the differential diagnosis of big toe pain, are not viewed from the perspective of MPS.

In ultrasound-guided dry needling of the flexor hallucis brevis muscle; the patient is placed in a supine position with the hip in external rotation and the knee in 90º flexion. It is important to use ultrasound guidance to protect the joints, nerves and vessels in the application area from possible damage. The ultrasound probe is placed perpendicular to the plantar axis. Needling is performed using the out of plane technique. A 0.25x25 mm needle is used (fig 1). The muscle is needled with the peppering method. Although there is no consensus in the literature, dry needling treatment is recommended to be performed once a week for a total of 3 sessions. It should also be noted that MPS can be a condition that can cause pain on its own, or it can be an entity accompanying another pathology.

References

1. Gilheany MF, Landorf KB, Robinson P. Hallux valgus and hallux rigidus: a comparison of impact on health-related quality of life in patients presenting to foot surgeons in Australia. J Foot Ankle Res 2008;1:1-6.
2. Abhishek A, Roddy E, Zhang W, Doherty M. Are hallux valgus and big toe pain associated with impaired quality of life? A cross-sectional study. Osteoarthritis Cartilage 2010;18:923-926.
3. Graff-Radford SB: Myofascial pain: diagnosis and management. Curr Pain Headache Rep 2004;8:463-467.
4. Travell JG, Simons DG. Myofascial pain and dysfunction: the trigger point manual. Lippincott Williams & Wilkins, 1992.
5. Yıldızgören M, Bağcıer F. Miyofasiyal ağri sendromu ve kuru iğneleme Kas, Tendon, Ligament ve Fasyaların Manuel Palpasyon Tekniğiyle ve Ultrason Rehberliğinde Kuru İğnelemesi 2022.

Intramural ectopic pregnancy at 21 weeks of gestation

Yuting Wei, Jin Wang, Hong Luo

Department of Ultrasound, West China Second University Hospital, Sichuan University, Key Laboratory of Birth Defects and Related Diseases of Women and Children (Sichuan University), Ministry of Education, Chengdu, China

To the Editor,

A 25-year-old woman (G1P0), at 21 6/7 weeks gestation, presented with severe lower abdominal pain. The patient had a laparoscopic myomectomy (9x8 cm) eight years earlier. A previous ultrasound (US) that the patient underwent showed an intrauterine pregnancy with no acute abnormalities. Urgent US demonstrated a large volume of hemoperitoneum. About 20 ml of incoagulable blood was extracted from her right middle abdomen. The patient was consented for emergency laparotomy and rupture of the posterior uterine wall was observed intraoperatively. The pregnancy was not communicated with the endometrial cavity and fallopian tubes, which was consistent with intramural ectopic pregnancy. A still-

Received 04.01.2023 Accepted 29.01.2023
Med Ultrason
2023, Vol. 25, No 1, 117-118, DOI: 10.11152/mu-4033,
Corresponding author: Prof. Hong Luo, Department of Ultrasound, West China Second University Hospital, No. 20, Section 3, South Renmin Road, Chengdu, Sichuan Province 610041, China
E-mail: luohongcd1969@163.com

birth was removed and uterine-conserving surgery was performed. The patient went home in stable condition on postoperative day 7.

Retrospective review of US images of the patient was performed. Ultrasonography at 6 1/7 weeks gestation showed the gestational sac was located within 5 mm of the uterine serosa (fig 1a). Ultrasonography at 12 0/7 weeks gestation presented the loss of clear zone under the placental bed, which was a sign of placenta accreta spectrum (fig 1b). Color Doppler ultrasonography at 21 5/7 weeks gestation presented retroplacental hypervascularity and thin myometrium between the endometrium and the amniotic sac (fig 1c). The postoperative pathology reported that villi invaded posterior myometrium (fig 1d).

Intramural ectopic pregnancy is the rarest form of ectopic pregnancy, accounting for less than 1% of ectopic pregnancies. It refers to a gestational sac surrounded by the uterine wall without connection to the endometrial cavity and fallopian tubes [1]. The risk of rupture of intramural pregnancy increases with the increase of the gestational age. Uterine trauma caused by surgical procedures including myomectomy, dilatation and curettage are predisposing factors for intramural ectopic pregnancy [2]. The treatment depends on the location and size of the gestational sac, the extent of myometrial involvement, gestational age at diagnosis and future fertility intentions [3]. Although intramural pregnancy is a rare form of ectopic pregnancy, early diagnosis is essential for the prevention of severe hemorrhage and loss of reproductive function.

Acknowledgement: this work was supported by the Sichuan Science and Technology Plan Project (Grant No. 2022YFS0086)

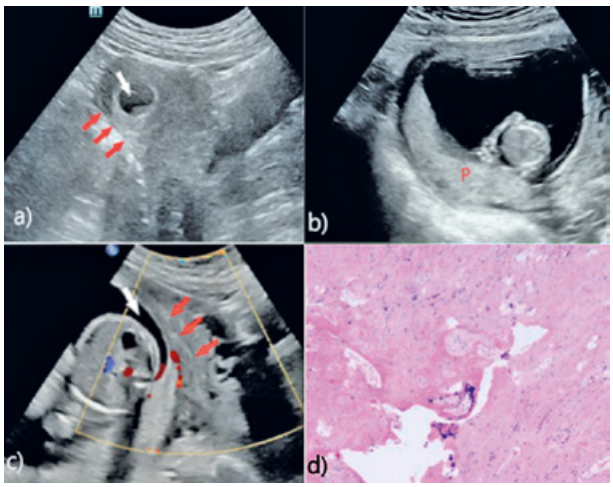

Fig 1. a) Greyscale and color Doppler ultrasonography images at 6 1/7 weeks of gestation. Gestational sac (white arrow), located within 5 mm of the uterine serosa (red arrow). b) Ultrasonography image at 12 0/7 weeks gestation presented the loss of clear zone under the placental bed. (P) placenta. c) Color Doppler ultrasonography at 21 5/7 weeks gestation showed thin myometrium between the endometrium (red arrow) and the amniotic sac (white arrow). d) Postoperative pathology showed that villi invaded posterior myometrium.

References

1. Zhang Q, Xing X, Liu S, et al. Intramural ectopic pregnancy following pelvic adhesion: case report and literature review. Arch Gynecol Obstet 2019;300:1507-1520.
2. Chaikof M, Hobson S, Sobel M. Fundal intramural ectopic pregnancy. CMAJ 2020;192:E1211.
3. Shen Z, Liu C, Zhao L, et al. Minimally-invasive management of intramural ectopic pregnancy: an eight-case series and literature review. Eur J Obstet Gynecol Reprod Biol 2020;253:180-186.

Ultrasound imaging and guided intervention for the middle cluneal nerve

Wei-Ting Wu[1,2], Yu-Chun Hsu1, Kamal Mezian[3], Vincenzo Ricci[4], Ke-Vin Chang[1,2,5], Levent Özçakar[6]

[1]Department of Physical Medicine and Rehabilitation, National Taiwan University Hospital, Bei-Hu Branch, Taipei, Taiwan,[2]Department of Physical Medicine and Rehabilitation, National Taiwan University College of Medicine, Taipei, Taiwan, [3]Department of Rehabilitation Medicine, First Faculty of Medicine and General University Hospital, Charles University in Prague, Prague, Czech, [4]Physical and Rehabilitation Medicine Unit, Luigi Sacco University Hospital, ASST Fatebenefratelli- Sacco, Milan, Italy, [5]Center for Regional Anesthesia and Pain Medicine, Wang-Fang Hospital, Taipei Medical University, Taipei, Taiwan, [6]Department of Physical and Rehabilitation Medicine, Hacettepe University Medical School, Ankara, Turkey

To the Editor,

A 55-year-old female suffered from right lower back and gluteal pain for the last year. Her symptoms aggravated after prolonged sitting and walking. Physical examination revealed tenderness with tingling sensation over the right sacroiliac joint (SIJ). Plain pelvic radiography showed normal bony alignment. As the pain could not be relieved by physical therapy, oral medication, and corticosteroid injection in the SIJ, she was referred for ultrasound-guided middle cluneal nerve (MCN) block (fig 1A). The transducer was first placed on the right SIJ parallel to the 2nd sacral foramina (fig 1B). Then the medial end of the transducer was pivoted caudally toward the lateral sacral crest (fig 1C). The MCN could be seen axially, inside the long posterior sacroiliac ligament (LPSL). Betamethasone (1 ml, 4 mg) mixed with lidocaine (2 ml, 1%) was administered using the in-plane approach to target the nerve branches (fig 1D, Video 1, on the journal site). The second injection was given two weeks later, and she described total pain relief thereafter.

The MCNs are derived from the dorsal rami of the sacral nerves S1-S3. The nerves exit the sacral foramina, piercing [1] or running superficial to [2] the LPSL between the posterior superior and posterior inferior iliac spines. They supply the cutaneous sensation of the medial aspect of gluteus maximus muscle. The average width of the MCNs in cadaveric specimens is 1.6 mm [3] when traveling into the LPSL. There are three common causes of MCN injury: LPSL sprain, iatrogenic injury during SIJ injection, and overstretching of the gluteus maximus.

In patients with MCN entrapment, pain can develop around the SIJ with possible radiation to the lower back, gluteus, and lower extremity [4]. Tenderness can be reproduced when pressure is applied inferolateral to the LPSL or 35 mm caudal to the posterior superior iliac spine [5]. Since the MCNs can be identified using the high-frequency transducer placed between the posterior superior iliac spine and lateral sacral crest, whereas ultrasound-guided injection can be used for a diagnostic/therapeutic block. Lastly, if synovitis/arthritis of the SIJ is present, the underlying disease should also be thoroughly managed to avoid recurrent entrapment.

Acknowledgment: The study was made possible by (1) the research funding of the Community and Geriatric Medicine Research Center, National Taiwan University Hospital, Bei-Hu Branch, Taipei, Taiwan; (2) Ministry of Science and Technology (MOST 106-2314-B-002-180-MY3, 109-2314-B-002-114-MY3 and 109-2314-B-002-127), and (3) Taiwan Society of Ultrasound in Medicine.

References

1. Aota Y. Entrapment of middle cluneal nerves as an unknown cause of low back pain. World J Orthop 2016;7:167-170.

Received 01.04.2022 Accepted 29.01.2023
Med Ultrason
2023, Vol. 25, No 1, 119-120, DOI: 10.11152/mu-4032,
Corresponding author: Ke-Vin Chang
Department of Physical Medicine and Rehabilitation, National Taiwan University Hospital Bei-Hu Branch, No. 87, Nei-Jiang Rd., Wan-Hwa District, Taipei 108, Taiwan
E-mail: kvchang011@gmail.com
Phone: +886223717101-5309

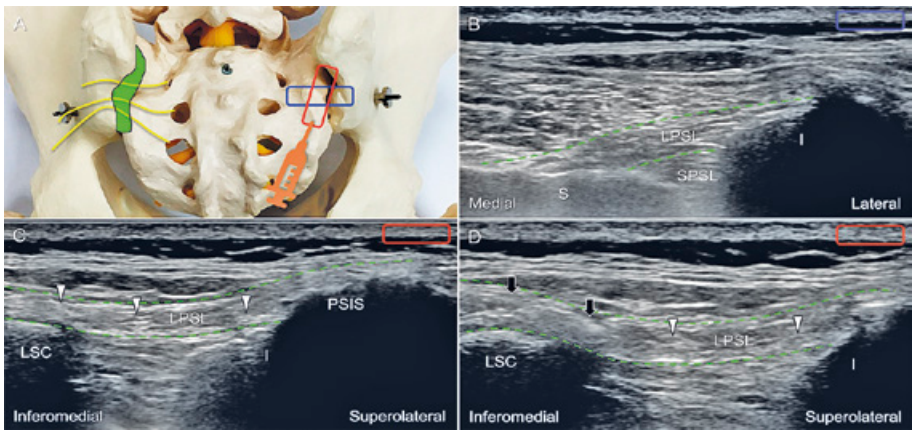

Fig 1. The schematic drawing shows the course of the middle cluneal nerves (A). The transducer is first placed on the sacroiliac joint (B), and then its medial end is pivoted 90 degrees caudally, toward the lateral edge of the sacral crest (C). The needle is inserted using the in-plane approach to target the middle cluneal nerves in the short-axis (D). Yellow line and white arrowheads: branches of the middle cluneal nerve; black arrows: needle; green shade and green dashed lines: long posterior sacroiliac ligament. S: sacrum; I: ilium; LPSL: long posterior sacroiliac ligament; SPSL: short posterior sacroiliac ligament; PSIS: posterior superior iliac spine; LSC: lateral edge of the sacral crest.

2. Tubbs RS, Levin MR, Loukas M, Potts EA, Cohen-Gadol AA. Anatomy and landmarks for the superior and middle cluneal nerves: application to posterior iliac crest harvest and entrapment syndromes. J Neurosurg Spine 2010;13:356-359.
3. Konno T, Aota Y, Saito T, et al. Anatomical study of middle cluneal nerve entrapment. J Pain Res 2017;10:1431-1435.
4. Karri J, Singh M, Orhurhu V, Joshi M, Abd-Elsayed A. Pain Syndromes Secondary to Cluneal Nerve Entrapment. Curr Pain Headache Rep 2020;24:61.
5. Matsumoto J, Isu T, Kim K, Iwamoto N, Morimoto D, Isobe M. Surgical treatment of middle cluneal nerve entrapment neuropathy: technical note. J Neurosurg Spine 2018;29:208-213.

Ultrasonographic and pathological findings of a secretory carcinoma of the parotid gland

Xiaowei Zhang[1], Dandan Wu[1], Jun Chen[2]

[1]Department of Pathology, [2]Department of Imaging Medicine, Affiliated Dongyang Hospital of Wenzhou Medical University, Dongyang, Zhejiang, P.R. China

Dear Editor,

A 48-year-old male patient was admitted because of a posterior right ear mass, which was first noted by the patient 2 months prior to admission as a broad, bean-sized mass. The patient did not report associated pain or facial numbness. A 1.0×1.0 cm mass was found behind the right ear; it was mobile with clear boundaries and was not associated with redness or tenderness. No swelling was noted in the lymph nodes of the neck.

Ultrasonography revealed a hypoechoic nodule in the right parotid gland, approximately 14×11×11 mm in size, with a well-defined border and an uneven internal echo. An irregular dark liquid area was present. Color Doppler flow imaging detected a few blood flow signals (fig 1a, 1b). Postoperative pathology after surgical resection confirmed the diagnosis of secretory carcinoma of the right parotid gland with immunohistochemistry: CK7+,

Received 21.11.2022 Accepted 29.01.2023
Med Ultrason
2023, Vol. 25, No 1, 120-121, DOI: 10.11152/mu-3962,
Corresponding author: Jun Chen
Department of Imaging Medicine, Dongyang Hospital Affiliated with Wenzhou Medical University, No. 60 West Wuning Road, Dongyang, Zhejiang, 322100, P.R. China
Phone/fax: +86 18868579300
+86 057989605211
E-mail: 547635310@qq.com

CK19+, S-100+, CK20+, SMA-, Desmin-, P63-, DOG-1-, Mammaglobin+, and Ki-67 (+, 5%) (fig 1c, 1d).

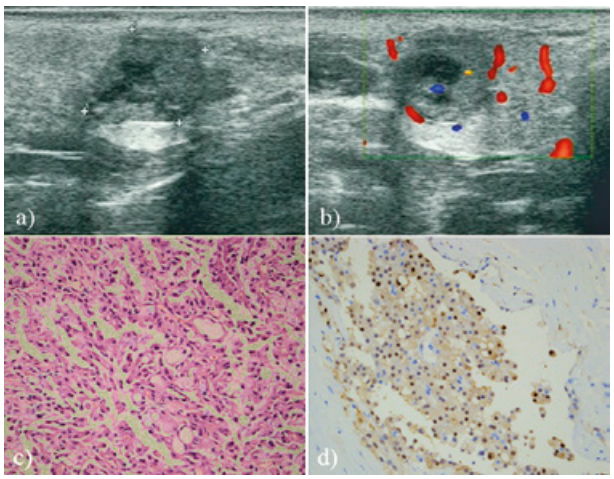

Fig 1. a) A hard hypoechoic nodule is visible in the right parotid gland. b) A few blood flow signals are seen on color Doppler flow imaging; c) The tumor displays a microcystic and papillary structure, with small to medium-large cells containing abundant and eosinophilic cytoplasm (Hematoxylin and Eosin stain ×200); d) Tumor cells are positive for S100 (Immunohistochemistry ×200).

Parotid secretory carcinomas are salivary gland tumors morphologically similar to those seen in breast secretory carcinomas and harbor a specific ETV6-NTRK3 fusion [1]. Secretory carcinomas of the parotid gland are usually characterized by occurring singularly, with different lesion locations and poor blood supply. They have been misdiagnosed as benign tumors of the parotid gland, as they present as a solid hypoechoic nodule that lacks the sonographic characteristics of typical parotid gland malignancy.

Parotid secretory carcinomas are usually low-grade malignancies and have relatively good prognoses. Local recurrence and local lymph node metastasis may occur, but distant metastasis is rare [2]. The first-line treatment option is the complete surgical resection of the tumor, followed by local radiotherapy.

References

1. Min FH, Li J, Tao BQ, et al. Parotid mammary analogue secretory carcinoma: a case report and review of literature. World J Clin Cases 2021;9:4052-4062.
2. Forner D, Bullock M, Manders D, et al. Secretory carcinoma: the eastern Canadian experience and literature review. J Otolaryngol Head Neck Surg 2018;47:69.